Frequency response of nonlinear oscillations of air column in a tube with an array of Helmholtz resonators

N. Sugimoto, M. Masuda, and T. Hashiguchi
Department of Mechanical Science, Graduate School of Engineering Science, University of Osaka, Toyonaka, Osaka 560-8531, Japan

(Received 10 January 2003; revised 20 June 2003; accepted 23 June 2003)

Nonlinear cubic theory is developed to obtain a frequency response of shock-free, forced oscillations of an air column in a closed tube with an array of Helmholtz resonators connected axially. The column is assumed to be driven by a plane piston sinusoidally at a frequency close or equal to the lowest resonance frequency with its maximum displacement fixed. By applying the method of multiple scales, the equation for temporal modulation of a complex pressure amplitude of the lowest mode is derived in a case that a typical acoustic Mach number is comparable with the one-third power of the piston Mach number, while the relative detuning of a frequency is comparable with the quadratic order of the acoustic Mach number. The steady-state solution gives the asymmetric frequency response curve with bending (skew) due to nonlinear frequency upshift in addition to the linear downshift. Validity of the theory is checked against the frequency response obtained experimentally. For high amplitude of oscillations, an effect of jet loss at the throat of the resonator is taken into account, which introduces the quadratic loss to suppress the peak amplitude. It is revealed that as far as the present check is concerned, the weakly nonlinear theory can give quantitatively adequate description up to the pressure amplitude of about 3% to the equilibrium pressure. [DOI: 10.1121/1.1600719]

PACS numbers: 43.25.Gf, 43.25.Vt, 43.25.Cb [MFH]

I. INTRODUCTION

Novel methods for generation of shock-free, high-amplitude oscillations of gas in a tube (or a container) have recently attracted much attention in view of applications to thermoacoustic devices. They commonly exploit resonance in one form or another by exciting an acoustic system at a frequency close to or equal to one of its resonance frequencies (eigenfrequencies). As the amplitude of oscillations of gas becomes high, however, there emerges a shock, i.e., discontinuity in pressure, etc., so that increase in pressure amplitude of oscillations tends to be suppressed as the excitation is increased.

Whether or not the shock emerges is crucially determined by the relation between resonance frequencies and frequencies of higher harmonics of the excitation. If the resonance frequencies are ordered as multiples of the fundamental one, just as in the case of a closed tube of uniform cross section, then the tube is called being *consonant* and otherwise *dissonant*.[1,2] As the amplitude of excitation is increased in a consonant tube, each frequency of higher harmonics generated by nonlinearity hits the respective resonance frequencies so that higher modes are gradually excited and energy in the fundamental mode is pumped up into higher modes and dissipated there. This cascade process of energy flow is the mechanisms behind emergence of the shock and the resulting suppression of increase in pressure amplitude of the fundamental mode.

In order to annihilate the shock, the cascade process should be blocked by any means. At present, there are two methods confirmed experimentally at high pressure level. One is the method devised by Lawrenson *et al.*[2] and Ilinskii *et al.*[3] at MacroSonix. The essential point lies in making the axial cross section of a container nonuniform so as to render it dissonant. By vibrating the whole container on a shaker, shock-free, high-amplitude oscillations have been achieved experimentally and theoretical analysis has also been made.

The other method is to exploit wave dispersion, as devised by the present authors,[4] although it was proposed originally in a different problem.[5] Sound speed in gas is usually constant independent of frequency; therefore, no dispersion occurs in propagation. But, by connecting external agents to the tube, the phase speed can be made dependent on a frequency. In fact, this is achieved by connecting an array of Helmholtz resonators to a tube of uniform cross section axially. By sinusoidally driving the bellows mounted at one end of this tube, shock-free, high-amplitude oscillations of about 10% of the equilibrium pressure have been generated at the other closed end. Because the phase speed now depends on the frequency, resonance frequencies are no longer ordered as multiples of the fundamental one, and the tube becomes dissonant automatically without any change of cross section of the tube.

In the present context, it may be worthwhile to mention the dispersion. For propagation in a tube of nonuniform cross section, the phase speed cannot be defined strictly even in the case of an exponential horn because the amplitude decays or grows in the direction of propagation. The propagation speed is then determined by the characteristics and is still given by the sound speed. In this sense, the system still remains *hyperbolic*. In the tube with the array, on the contrary, a plane sinusoidal wave can be propagated so that the phase speed is clearly defined, which is now different from the sound speed and dependent on the frequency. The connection of the array changes the hyperbolic system originally to be *dispersive*.

 0001-4966/2003/114(4)/1772/13/$19.00

Besides the two methods, Rudenko *et al.*[6] have already proposed ideas to block the cascade process by introducing special absorbers of the second harmonics through the boundary condition. Andreev *et al.*[7] have confirmed the effects experimentally, though at even lower pressure level. For suppression or reduction of the second harmonics, Gusev *et al.*[8] have abandoned a usual monochromatic excitation to control the driver actively by adding to the fundamental sinusoidal excitation the second harmonic one with a phase difference. While these methods focus on increase in so-called *quality factor* of a resonator, it is questionable whether or not shock-free oscillations are ultimately achieved.

The purpose of this paper is to formulate nonlinear forced oscillations of an air column in the tube with the array of Helmholtz resonators and to derive theoretically a frequency response corresponding to the one obtained experimentally.[4] Supposing each resonator is small in effect, one-dimensional motion of air is assumed over the cross section of the tube except for a boundary layer on the wall and vicinity of resonator's orifices open to the tube. Supposing also that the axial spacing between neighboring resonators is small in comparison with a wavelength, the continuum approximation for the resonators is made so that the effects of the discrete distribution in array may be smeared out per axial length.

Because the pressure level observed in the experiment is still small relative to the equilibrium pressure, weakly nonlinear theory is developed by using the asymptotic method of multiple (two) scales.[9] The bellows used in the experiment are modeled as a plane piston reciprocating sinusoidally by taking account of the correspondence between the displacement of the bellows and the one of the piston. The boundary condition for the piston is usually of three types, either one of the maximum displacement, maximum speed, or maximum acceleration being held constant, the first of which is used in the present theory.

As the ratio of the maximum displacement of the piston to the tube length is much smaller than unity, so is the piston Mach number defined by the ratio of the maximum piston speed to the sound speed, which is comparable in order with the former. Denoting the piston Mach number by ε_p, and a typical acoustic Mach number in the tube by ε, respectively, the situation in the experiment corresponds to a case where ε is of order $\varepsilon_p^{1/3}$ and the relative detuning of a frequency from the resonance one is of order ε^2 $(=\varepsilon_p^{2/3})$. It is emphasized that the rigorous cubic nonlinear theory starting from the formulation based on the above assumptions is necessary to obtain a frequency response correctly up to the third order in the pressure amplitude.

The problem is formulated in Sec. II and the lossless linear theory is first described in Sec. III. Section IV is devoted to the nonlinear theory by using the method of multiple scales to derive the equation for slow modulation of a complex pressure amplitude of the fundamental mode. From the steady-state solution to the equation, the frequency response is obtained and compared with the experiment. In Sec. V, an effect of the jet loss at the throat of the resonator is considered in order to compensate the discrepancy between the theory and experiment as the amplitude becomes high.

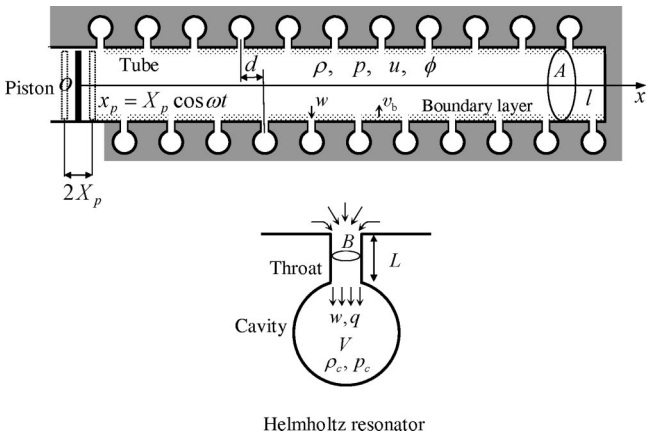

FIG. 1. Illustration of a tube with an array of Helmholtz resonators.

II. FORMULATION OF THE PROBLEM

A. Basic equations

We start by formulating the problem. Suppose a straight, rigid tube of radius R and of length l, to which an array of Helmholtz resonators is connected (see Fig. 1). One end of the tube is allowed to be displaced by a plane piston while the other end is closed by a flat plate. The tube is closed hermetically with the resonators inclusive. Each resonator is assumed small in the sense that the cavity's volume V is much smaller than the tube's volume per spacing Ad, A $(=\pi R^2)$ being the cross-sectional area of the tube and d the axial spacing. This ratio is denoted by κ $(\equiv V/Ad \ll 1)$, and called a *size parameter* of the array. Taking the axial spacing to be much smaller than a wavelength of oscillation, the continuum approximation is made for discrete distribution of the resonators to average its effect per unit axial length.

The Reynolds number is usually sufficiently high that effects of viscosity and heat conduction are limited only within the boundary layer developing on the tube wall. In the outside of the boundary layer called a region of an acoustic main flow, these lossy effects are negligible. The boundary layer is thin and the array is small $(\kappa \ll 1)$, so the acoustic main flow may be regarded as being almost one-dimensional. Under these assumptions, the basic equations for the main flow have already been presented in Ref. 10.

The equations of continuity and of motions are combined into the following equations:

$$\left[\frac{\partial}{\partial t}+(u\pm a)\frac{\partial}{\partial x}\right]\left[u\pm\frac{2}{\gamma-1}(a-a_0)\right]=\pm\frac{a}{A}\oint v_n\,\mathrm{d}s, \tag{1}$$

with the signs ordered vertically where x and t denote, respectively, the axial coordinate along the tube and the time, while u and a denote, respectively, the axial velocity of the air and the local sound speed. The latter is defined by

$$a^2=\frac{\mathrm{d}p}{\mathrm{d}\rho}=a_0^2\left(\frac{p}{p_0}\right)^{(\gamma-1)/\gamma}, \tag{2}$$

with $a_0=\sqrt{\gamma p_0/\rho_0}$ where p and ρ denote, respectively, the pressure and density of the air and the subscript 0 attached to p and ρ implies the respective values in equilibrium, γ being the ratio of the specific heats, and a_0 is the linear sound speed. Since the lossy effects are neglected in the acoustic main flow, the adiabatic relation $p/p_0=(\rho/\rho_0)^\gamma$ is assumed to hold.

Through the right-hand side of (1) are included the effects of the boundary layer and of the array of Helmholtz resonators. Here, v_n represents the velocity directed inward normal to the boundary of the axial cross section of the acoustic main-flow region, ds being the line element along the boundary. Where the tube wall exists, v_n is the velocity at the edge of the boundary layer v_b, given by

$$v_b=\left(1+\frac{\gamma-1}{\sqrt{\mathrm{Pr}}}\right)\sqrt{\nu}\,\frac{\partial^{-1/2}}{\partial t^{-1/2}}\left(\frac{\partial u}{\partial x}\right), \tag{3}$$

where ν denotes the kinematic viscosity taken constant, Pr being the Prandtl number, and the derivative of minus half-order of a function $f(x,t)$ is defined as

$$\frac{\partial^{-1/2}f}{\partial t^{-1/2}}\equiv\frac{1}{\sqrt{\pi}}\int_{-\infty}^{t}\frac{f(x,\tau)}{\sqrt{t-\tau}}\,\mathrm{d}\tau. \tag{4}$$

On the other hand, where the tube opens to the resonator, v_n is the velocity of the air flowing out of the throat into the tube, $-w$. Because the throat is much shorter than a typical wavelength, the mass flux density q averaged over the cross section of the throat may be regarded as being uniform along the throat. While no account of motions of the air is taken in the cavity, the rate of increase in the mass therein must balance with the mass flux flown into it. This requires that

$$V\frac{\partial\rho_c}{\partial t}=Bq, \tag{5}$$

where ρ_c denotes the mean density of the air in the cavity, and B denotes the cross-sectional area of the throat.

Thus, the integral in (1) consists of two contributions as follows:

$$\frac{1}{A}\oint v_n\,\mathrm{d}s=2\left(1+\frac{\gamma-1}{\sqrt{\mathrm{Pr}}}\right)\frac{\sqrt{\nu}}{R^*}\,\frac{\partial^{-1/2}}{\partial t^{-1/2}}\left(\frac{\partial u}{\partial x}\right)-\frac{\kappa}{\rho}\,\frac{\partial\rho_c}{\partial t}, \tag{6}$$

where R^* is the reduced radius of the tube defined by $R/(1-BR/2Ad)$, and q is set equal to ρw at the orifice on the tube side. The derivation of the right-hand side of (6) may be facilitated by multiplying A and ds by d, respectively, noting that $d(\mathrm{d}s)$ corresponds to the area element on the surface bounding the region of the acoustic main flow. Here, q in (5) is expressed in terms of the excess pressure p_c' $(=p_c-p_0)$ in place of the density. Assuming the adiabatic relation for the air in the cavity, ρ_c is expanded into the Taylor series with respect to p_c' to yield q in the following form:

$$q=\frac{V}{Ba_0^2}\,\frac{\partial}{\partial t}\left[p_c'-\frac{(\gamma-1)}{2\gamma p_0}p_c'^2+\frac{(\gamma-1)(2\gamma-1)}{6\gamma^2p_0^2}p_c'^3+\cdots\right]. \tag{7}$$

The behavior of the resonator is governed by (5) supplemented by the equation of motion for the air in the throat. The momentum balance of the air in the throat of length L requires that

$$L\frac{\partial q}{\partial t}=-p_c+p-\frac{2L\sqrt{\nu}}{r}\,\frac{\partial^{1/2}}{\partial t^{1/2}}(\rho_0 w), \tag{8}$$

where the last term represents the friction at the throat wall.[10] Using the lowest relation of (7) to evaluate $\rho_0 w$, substitution of (7) for q into (8) leads to the following equation:

$$\begin{aligned}\frac{\partial^2p_c'}{\partial t^2}+\frac{2\sqrt{\nu}}{r^*}\,\frac{\partial^{3/2}p_c'}{\partial t^{3/2}}+\omega_0^2p_c'&=\omega_0^2p'+\frac{\gamma-1}{2\gamma p_0}\,\frac{\partial^2p_c'^2}{\partial t^2}-\frac{(\gamma-1)(2\gamma-1)}{6\gamma^2p_0^2}\,\frac{\partial^2p_c'^3}{\partial t^2}\\&\quad+\cdots,\end{aligned} \tag{9}$$

where p' $(=p-p_0)$ is the excess pressure in the tube, r^* $(=r/c_L)$, c_L being L'/L_e with $L'=L+2r$ and $L_e=L+2\times0.82r$, is the reduced radius of the throat by taking account of the end corrections on both ends, and ω_0 $(=\sqrt{Ba_0^2/L_eV})$ is the natural angular frequency of the resonator.[4] The derivative of three-half order is defined by differentiating the derivative of minus half-order twice with respect to t.

B. Reduction by the velocity potential

Addition and subtraction of (1) with the upper and lower signs lead, respectively, to

$$\frac{\partial u}{\partial t}+u\frac{\partial u}{\partial x}+\frac{2a}{\gamma-1}\,\frac{\partial a}{\partial x}=0, \tag{10}$$

and

$$\frac{2}{\gamma-1}\left(\frac{\partial a}{\partial t}+u\frac{\partial a}{\partial x}\right)+a\frac{\partial u}{\partial x}=\frac{a}{A}\oint v_n\,\mathrm{d}s. \tag{11}$$

In order to eliminate a from these equation, we introduce a velocity potential ϕ defined by

$$u\equiv\frac{\partial\phi}{\partial x}. \tag{12}$$

Substituting (12) into (10) and integrating this with respect to x, we have

$$a^2=a_0^2-(\gamma-1)\left[\frac{\partial\phi}{\partial t}+\frac{1}{2}\left(\frac{\partial\phi}{\partial x}\right)^2\right]. \tag{13}$$

This is simply the Bernoulli's theorem. Multiplying (11) by a and using (13) to eliminate a^2, we derive

$$\frac{\partial^2\phi}{\partial t^2}-a_0^2\frac{\partial^2\phi}{\partial x^2}=-\frac{\partial}{\partial t}\left(\frac{\partial\phi}{\partial x}\right)^2-(\gamma-1)\frac{\partial\phi}{\partial t}\frac{\partial^2\phi}{\partial x^2}-\frac{\gamma+1}{2}\left(\frac{\partial\phi}{\partial x}\right)^2\frac{\partial^2\phi}{\partial x^2}-\frac{a^2}{A}\oint v_n\,\mathrm{d}s. \tag{14}$$

In passing, substituting (13) into (2), p' is expressed inversely in terms of ϕ. In fact, by expanding $p/p_0=(a^2/a_0^2)^{\gamma/(\gamma-1)}$ around $a=a_0$ and truncating the series at the cubic terms, it follows that

$$p'=-\rho_0\frac{\partial\phi}{\partial t}+\frac{\rho_0}{2a_0^2}\left[\left(\frac{\partial\phi}{\partial t}\right)^2-a_0^2\left(\frac{\partial\phi}{\partial x}\right)^2\right]+\frac{\rho_0}{2a_0^2}\left[\frac{(\gamma-2)}{3a_0^2}\left(\frac{\partial\phi}{\partial t}\right)^3+\frac{\partial\phi}{\partial t}\left(\frac{\partial\phi}{\partial x}\right)^2\right]+\cdots. \tag{15}$$

The boundary conditions are imposed at the piston surface and the closed end so that the velocity of the air may be equal to the one of the respective surfaces. Taking the origin of the coordinate x at the mean position of the piston surface over one period and the closed end at $x=l$, the respective conditions are expressed as follows:

$$\frac{\partial\phi}{\partial x}=\frac{\mathrm{d}x_p}{\mathrm{d}t}=\frac{i}{2}\omega X_p\mathrm{e}^{i\omega t}+\text{c.c.}$$

$$\text{at}\quad x=x_p=\frac{1}{2}X_p\mathrm{e}^{i\omega t}+\text{c.c.}=X_p\cos(\omega t), \tag{16}$$

and

$$\frac{\partial\phi}{\partial x}=0\quad\text{at}\quad x=l, \tag{17}$$

where x_p denotes the position of the piston surface; the displacement amplitude, X_p, and the angular frequency of excitation, ω, are taken real and positive, c.c. implying the complex conjugate to *all preceding terms*, if any.

C. Normalization

We next normalize the equations and the boundary conditions by making the following replacement:

$$[x,\ t,\ \phi,\ a,\ \rho,\ \rho_c,\ p',\ p_c']=[l\overline{x},\ (l/a_0)\overline{t},\ lu_0\overline{\phi},\ a_0\overline{a},\ \rho_0\overline{\rho},\ \rho_0\overline{\rho_c},\ \rho_0a_0u_0\overline{p'},\ \rho_0a_0u_0\overline{p_c'}], \tag{18}$$

where the quantities with the overbar imply the dimensionless ones, and u_0 is a typical speed of the air, say the maximum speed in the acoustic main flow. Here, two Mach numbers are defined: one is the acoustic Mach number ε associated with the air speed and the other the piston Mach number ε_p. Both Mach numbers are assumed to be much smaller than unity, as

$$\varepsilon\equiv\frac{u_0}{a_0}\ll1\quad\text{and}\quad\varepsilon_p\equiv\frac{\omega X_p}{a_0}\ll1. \tag{19}$$

In a lossless case of a tube without the array of resonators, it is known that the air column will resonate in the lowest mode when a half-wavelength $\pi a_0/\omega$ coincides with the tube length. Using this angular frequency $\pi a_0/l$, ω is made dimensionless by introducing σ as

$$\omega=\frac{\pi a_0}{l}\sigma. \tag{20}$$

By the replacement (18), (14) with (6) is normalized as

$$\frac{\partial^2\overline{\phi}}{\partial\overline{t}^2}-\frac{\partial^2\overline{\phi}}{\partial\overline{x}^2}=\frac{\kappa\overline{a}^2}{\varepsilon\overline{\rho}}\frac{\partial\overline{\rho_c}}{\partial\overline{t}}-\varepsilon\left[\frac{\partial}{\partial\overline{t}}\left(\frac{\partial\overline{\phi}}{\partial\overline{x}}\right)^2+(\gamma-1)\frac{\partial\overline{\phi}}{\partial\overline{t}}\frac{\partial^2\overline{\phi}}{\partial\overline{x}^2}\right]-\varepsilon^2\frac{(\gamma+1)}{2}\left(\frac{\partial\overline{\phi}}{\partial\overline{x}}\right)^2\frac{\partial^2\overline{\phi}}{\partial\overline{x}^2}-\delta\overline{a}^2\frac{\partial^{-1/2}}{\partial\overline{t}^{-1/2}}\left(\frac{\partial^2\overline{\phi}}{\partial\overline{x}^2}\right), \tag{21}$$

with $\overline{\rho}=(1+\varepsilon\gamma\overline{p}')^{1/\gamma}$, $\overline{\rho_c}=(1+\varepsilon\gamma\overline{p_c}')^{1/\gamma}$, and $\overline{a}^2=1-\varepsilon(\gamma-1)[\partial\overline{\phi}/\partial\overline{t}+\varepsilon(\partial\overline{\phi}/\partial\overline{x})^2/2]$, where $\overline{a}^2/\overline{\rho}$ and $\overline{\rho_c}$ are expanded, respectively, as

$$\frac{\overline{a}^2}{\overline{\rho}}=1-\varepsilon(\gamma-2)\frac{\partial\overline{\phi}}{\partial\overline{t}}-\varepsilon^2\frac{(\gamma-2)}{2}\left[\left(\frac{\partial\overline{\phi}}{\partial\overline{t}}\right)^2+\left(\frac{\partial\overline{\phi}}{\partial\overline{x}}\right)^2\right]+\cdots, \tag{22}$$

and

$$\overline{\rho_c}=1+\varepsilon\overline{p_c}'-\varepsilon^2\frac{(\gamma-1)}{2}\overline{p_c}'^2+\varepsilon^3\frac{(\gamma-1)(2\gamma-1)}{6}\overline{p_c}'^3+\cdots. \tag{23}$$

On the other hand, (9) is normalized as

$$\frac{\partial^2\overline{p_c}'}{\partial\overline{t}^2}+\delta_r\frac{\partial^{3/2}\overline{p_c}'}{\partial\overline{t}^{3/2}}+(\pi\sigma_0)^2\overline{p_c}'=(\pi\sigma_0)^2\overline{p}'+\varepsilon\frac{(\gamma-1)}{2}\frac{\partial^2\overline{p_c}'^2}{\partial\overline{t}^2}-\varepsilon^2\frac{(\gamma-1)(2\gamma-1)}{6}\times\frac{\partial^2\overline{p_c}'^3}{\partial\overline{t}^2}+\cdots, \tag{24}$$

with $\sigma_0=l\omega_0/\pi a_0$, where δ and δ_r are the parameters representing the boundary-layer effects due to the tube wall and the throat wall, respectively, and are given by

$$\delta=2\left(1+\frac{\gamma-1}{\sqrt{\mathrm{Pr}}}\right)\frac{\sqrt{\nu l/a_0}}{R^*}\quad\text{and}\quad\delta_r=2\frac{\sqrt{\nu l/a_0}}{r^*}. \tag{25}$$

In (24), $\overline{p}'$ is given, after normalization of (18), by

$$\overline{p}'=-\frac{\partial\overline{\phi}}{\partial\overline{t}}+\frac{\varepsilon}{2}\left[\left(\frac{\partial\overline{\phi}}{\partial\overline{t}}\right)^2-\left(\frac{\partial\overline{\phi}}{\partial\overline{x}}\right)^2\right]+\frac{\varepsilon^2}{2}\left[\frac{(\gamma-2)}{3}\left(\frac{\partial\overline{\phi}}{\partial\overline{t}}\right)^3+\frac{\partial\overline{\phi}}{\partial\overline{t}}\left(\frac{\partial\overline{\phi}}{\partial\overline{x}}\right)^2\right]+\cdots. \tag{26}$$

On the other hand, the boundary conditions are normalized as

$$\frac{\partial \bar{\phi}}{\partial \bar{x}} = i\frac{\pi\sigma c}{2\varepsilon} e^{i\pi\sigma\bar{t}} + \text{c.c. at } \bar{x} = \frac{c}{2} e^{i\pi\sigma\bar{t}} + \text{c.c.}, \tag{27}$$

and

$$\frac{\partial \bar{\phi}}{\partial \bar{x}} = 0 \text{ at } \bar{x} = 1, \tag{28}$$

where c represents the dimensionless amplitude X_p/l ($\ll 1$) and $\pi\sigma c$ corresponds to ε_p.

III. LOSSLESS LINEAR THEORY

At first, it is instructive to discuss the lossless linear case. Taking the limit as c, δ, and $\delta_r \to 0$, with c/ε fixed, the linearized problem is governed by the following equations:

$$\frac{\partial^2 \phi}{\partial t^2} - \frac{\partial^2 \phi}{\partial x^2} = \kappa \frac{\partial p_c'}{\partial t}, \tag{29}$$

$$\frac{\partial^2 p_c'}{\partial t^2} + (\pi\sigma_0)^2 p_c' = (\pi\sigma_0)^2 p', \tag{30}$$

$$p' = -\frac{\partial \phi}{\partial t}, \tag{31}$$

with the boundary conditions given by

$$\frac{\partial \phi}{\partial x} = i\frac{\pi\sigma c}{2\varepsilon} e^{i\pi\sigma t} + \text{c.c. at } x = 0 \text{ and } \frac{\partial \phi}{\partial x} = 0 \text{ at } x = 1. \tag{32}$$

Here and hereafter, the overbar is omitted.

Setting

$$\begin{bmatrix} \phi \\ p' \\ p_c' \end{bmatrix} = \begin{bmatrix} \Phi(x) \\ F(x) \\ G(x) \end{bmatrix} e^{i\pi\sigma t} + \text{c.c.}, \tag{33}$$

and substituting this into (29)–(31) to eliminate F and G, we derive

$$\frac{d^2\Phi}{dx^2} + k^2\Phi = 0, \tag{34}$$

where k is given by

$$k^2 = (\pi\sigma)^2\left(1 + \frac{\kappa\sigma_0^2}{\sigma_0^2 - \sigma^2}\right). \tag{35}$$

Imposing the boundary conditions (32), the solutions are easily obtained as

$$\begin{bmatrix} \phi \\ p' \\ p_c' \end{bmatrix} = \begin{bmatrix} i/\pi\sigma \\ 1 \\ s \end{bmatrix} \frac{\pi^2\sigma^2\cos[k(x-1)]}{k\sin k} \frac{c}{2\varepsilon} e^{i\pi\sigma t} + \text{c.c.}, \tag{36}$$

with $s = \sigma_0^2/(\sigma_0^2 - \sigma^2)$.

It is noted in (36) that k becomes purely imaginary for $\sigma_0 < \sigma < \sqrt{1+\kappa}\,\sigma_0$. Then, $\cos[k(x-1)]$ and $k\sin k$ take, respectively, $\cosh[|k|(x-1)]$ and $-|k|\sinh|k|$. As σ approaches σ_0, k tends to diverge and the evanescence occurs in the limit. This is due to the side-branch resonance where each resonator reflects back the incident wave totally. As σ approaches $\sqrt{1+\kappa}\,\sigma_0$, on the other hand, k tends to vanish.

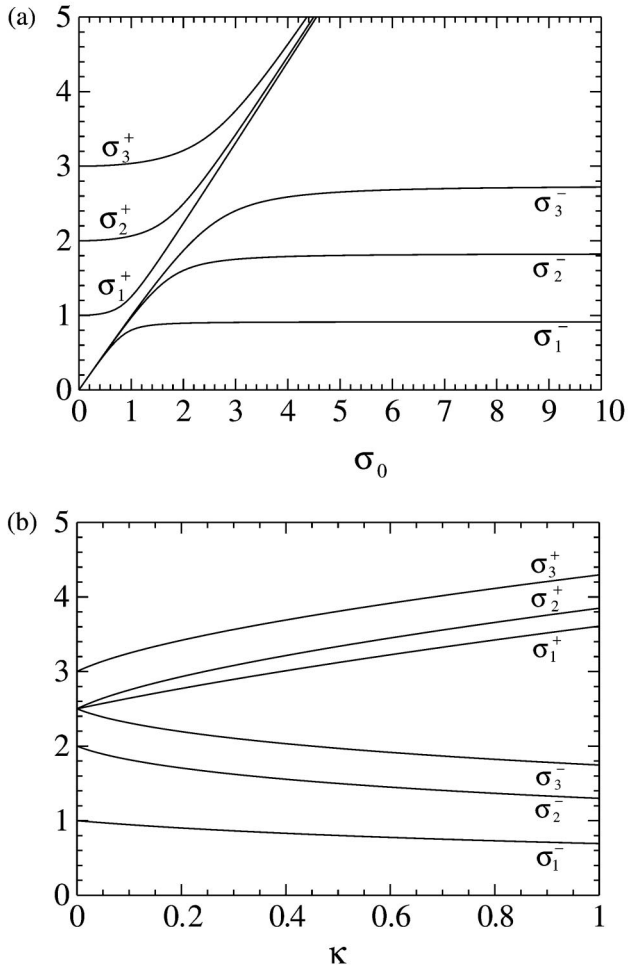

FIG. 2. Graphs of the resonance frequencies $\sigma_m^{\pm}$ ($m = 1$, 2, and 3): (a) displays the dependence on σ_0 with the value of κ fixed at 0.2, and (b) displays the dependence on κ with the value of σ_0 fixed at 2.5.

This is a resonance supported by the array of resonators where the air column oscillates in unison. It seems to be worth examining this new resonance, but we are concerned here with the resonance when $\sin k$ vanishes, i.e., $k = m\pi$ (>0) ($m = 1,2,3,\ldots$).

Unlike in the case of the tube without the array, there are two resonance frequencies $\sigma_m^{\pm}$ (>0) for a given value of m. They are determined from the quadratic equation $\sigma^4 - [m^2 + (1+\kappa)\sigma_0^2]\sigma^2 + m^2\sigma_0^2 = 0$ in σ^2 as

$$(\sigma_m^{\pm})^2 = \tfrac{1}{2}\{m^2 + (1+\kappa)\sigma_0^2 \pm \sqrt{[m^2 + (1+\kappa)\sigma_0^2]^2 - 4m^2\sigma_0^2}\}, \tag{37}$$

with the signs ordered vertically. It is easily found that $\sigma_m^- < \sigma_0 < \sqrt{1+\kappa}\,\sigma_0 < \sigma_m^+$. Figure 2 shows the dependence of $\sigma_m^{\pm}$ ($m = 1$, 2, and 3) on σ_0 or κ for either one fixed. In the tube without the array, the resonance frequencies are given by $\sigma = m$ simply. In Fig. 2(a), where κ is fixed to be 0.2, it is seen that σ_m^+ tends to m as σ_0 vanishes, whereas σ_m^- tends to vanish. On the other hand, as σ_0 becomes large, σ_m^+ and σ_m^- tend to $\sqrt{1+\kappa}\,\sigma_0$ and $m/\sqrt{1+\kappa}$, respectively, for $m \ll \sigma_0$. For a large value of σ_0, it is σ_m^-'s that correspond to the resonance frequencies in the tube without the array. But,

since the tube then becomes consonant, the merit of connection of the array is lost. For a fixed value of $\sigma_0=2.5$, on the other hand, the dependence of $\sigma_m^{\pm}$ on κ is shown in Fig. 2(b). As κ increases, the resonance frequencies σ_m^- decrease, whereas σ_m^+ increase. For a small value of κ, $\sigma_m^{\pm}$ are expressed asymptotically as

$$\sigma_m^+=\sigma_0\left[1+\frac{\kappa\sigma_0^2}{2(\sigma_0^2-m^2)}+\cdots\right], \tag{38}$$

and

$$\sigma_m^-=m\left[1-\frac{\kappa\sigma_0^2}{2(\sigma_0^2-m^2)}+\cdots\right], \tag{39}$$

for $\sigma_0>m$, while the expressions of $\sigma_m^{\pm}$ are exchanged for $\sigma_0<m$.

IV. NONLINEAR THEORY

We now develop a nonlinear theory by taking account of small but finite magnitude of ε and also lossy effects. While the magnitudes of c and of ε_p are defined clearly, the one of ε is left ambiguous and should now be related to c. When the driving frequency σ is off the resonance, the linear solution (36) suggests that ε is of the same order as c or ε_p. This is because the quantities on the left-hand side of (36) are regarded as being of order unity. But, as σ is set closer to the resonance frequency, ε becomes much larger than c, as the term ''resonance'' implies. Then, ε is determined not only by c but also by a detuning $\Delta\sigma$, indicating how far the driving frequency is set from the resonance one. Since the experiment exploits the resonance in the lowest mode, we consider a case where σ is near the lowest resonance frequency σ_1^- $(\equiv\sigma_1)$. Setting $\Delta\sigma=\sigma-\sigma_1$, $k\sin k$ in the denominator of (36) may be approximated as $-\pi(\mathrm{d}k/\mathrm{d}\sigma)|_{\sigma=\sigma_1}\Delta\sigma$, so ϕ, p', and p_c' are estimated to be of order $c/\varepsilon|\Delta\sigma|$. For this to be of order unity, ε is determined as

$$\varepsilon\approx\frac{c}{|\Delta\sigma|}. \tag{40}$$

Since we assume the lossless case here, ε diverges, of course, as $\Delta\sigma$ vanishes. The experimental result indicates that c is of order 10^{-3}, $|\Delta\sigma|$ is of 10^{-2}, and ε is of 10^{-1}. This suggests that c is of ε^3 and $\Delta\sigma$ is of ε^2. Also, δ and δ_r for the lossy effects are estimated to be of ε^2.

A. Perturbation procedures

In light of the ordering mentioned above, the exponential factor $\exp(i\pi\sigma t)$ in (27) may be written as $\exp[i\pi(\sigma_1+\varepsilon^2\sigma')t]$ by setting $\Delta\sigma=\varepsilon^2\sigma'$, σ' being a quantity of order unity. Regarding $\varepsilon^2 t$ as a slow variable compared with t, we employ the method of multiple (two) scales by introducing two variables t_0 $(\equiv t)$ and t_2 $(\equiv\varepsilon^2 t)$. Then, the boundary condition (27) may be given, without the overbar, as

$$\frac{\partial\phi}{\partial x}=i\frac{E}{2}\mathrm{e}^{i\pi\sigma_1 t_0}+\text{c.c.}+O(\varepsilon^2 E)$$

$$\text{at}\quad x=\frac{c}{2}\mathrm{e}^{i\pi\sigma_1 t_0}+\text{c.c.}+O(\varepsilon^2 c), \tag{41}$$

where we note that E $[=(\pi\sigma_1 c/\varepsilon)\exp(i\pi\sigma' t_2)]$ is dependent of t_2 and is of order ε^2.

We seek the solutions to (21) and (24) with (26) under the boundary conditions (41) and (28) in the asymptotic expansion of ε as

$$\begin{bmatrix}\phi\\ p'\\ p_c'\end{bmatrix}=\begin{bmatrix}\phi^{(0)}\\ f^{(0)}\\ g^{(0)}\end{bmatrix}+\varepsilon\begin{bmatrix}\phi^{(1)}\\ f^{(1)}\\ g^{(1)}\end{bmatrix}+\varepsilon^2\begin{bmatrix}\phi^{(2)}\\ f^{(2)}\\ g^{(2)}\end{bmatrix}+\cdots. \tag{42}$$

By introduction of t_2, the differential operator is expanded as

$$\frac{\partial}{\partial t}=\frac{\partial}{\partial t_0}+\varepsilon^2\frac{\partial}{\partial t_2}+\cdots. \tag{43}$$

The lowest-order problem of ε takes the same form as (29) to (31) with ϕ, p', and p_c' replaced by $\phi^{(0)}$, $f^{(0)}$, and $g^{(0)}$, respectively. But, they are now subjected to the homogeneous boundary conditions: $\partial\phi^{(0)}/\partial x=0$ at $x=0$ and $x=1$, since $\partial\phi/\partial x$ in (41) is expanded around $x=0$ and E is assumed to be of order ε^2. Thus, the lowest-order solutions are given by the eigensolutions of the system. Taking, in (36), the formal limit as $c/\varepsilon\to 0$, $k\to\pi$, and $\sigma\to\sigma_1$, and setting $(\pi^2\sigma^2/k\sin k)c/2\varepsilon$ to be α, the solutions are obtained as

$$\begin{bmatrix}\phi^{(0)}\\ f^{(0)}\\ g^{(0)}\end{bmatrix}=\begin{bmatrix}i/\pi\sigma_1\\ 1\\ s_1\end{bmatrix}\cos[\pi(x-1)]\alpha\mathrm{e}^{i\pi\sigma_1 t_0}+\text{c.c.}, \tag{44}$$

with $s_1=\sigma_0^2/(\sigma_0^2-\sigma_1^2)$ $(\sigma_1\neq\sigma_0)$, where $\pi^2\sigma_1^2(1+\kappa s_1)=\pi^2$ and the complex amplitude α including the detuning is assumed to depend on t_2 but unspecified at this order.

Here, we make the following remark. The constant s_1 becomes positive or negative depending on the values of σ_0 and σ_1. Therefore, the pressure in the cavity differs from the one in the tube in magnitude and phase. If σ_0 is chosen greater than σ_1, as is usually the case, the pressure amplitude in the cavity becomes higher than the one in the tube.

1. First-order problem

Let us now proceed to the first-order problem. Then, the equations take the following form:

$$\frac{\partial^2\phi^{(1)}}{\partial t_0^2}-\frac{\partial^2\phi^{(1)}}{\partial x^2}-\kappa\frac{\partial g^{(1)}}{\partial t_0}$$

$$=-\kappa\left[(\gamma-1)g^{(0)}+(\gamma-2)\frac{\partial\phi^{(0)}}{\partial t_0}\right]\frac{\partial g^{(0)}}{\partial t_0}$$

$$-\frac{\partial}{\partial t_0}\left(\frac{\partial\phi^{(0)}}{\partial x}\right)^2-(\gamma-1)\frac{\partial\phi^{(0)}}{\partial t_0}\frac{\partial^2\phi^{(0)}}{\partial x^2}, \tag{45}$$

and

$$\frac{\partial^2 g^{(1)}}{\partial t_0^2}+(\pi\sigma_0)^2 g^{(1)}-(\pi\sigma_0)^2 f^{(1)}=\frac{(\gamma-1)}{2}\frac{\partial^2 g^{(0)2}}{\partial t_0^2}, \tag{46}$$

with

$$f^{(1)}=-\frac{\partial\phi^{(1)}}{\partial t_0}+\frac{1}{2}\left(\frac{\partial\phi^{(0)}}{\partial t_0}\right)^2-\frac{1}{2}\left(\frac{\partial\phi^{(0)}}{\partial x}\right)^2, \tag{47}$$

while the boundary conditions at this order take simply

$$\frac{\partial\phi^{(1)}}{\partial x}=0 \quad \text{at} \quad x=0 \quad \text{and} \quad x=1. \tag{48}$$

Introducing (44) into the right-hand sides of (45)–(47), we find the first-order solutions should be in the following form:

$$\begin{bmatrix}\phi^{(1)}\\ f^{(1)}\\ g^{(1)}\end{bmatrix}=\begin{bmatrix}\Phi_2^{(1)}\\ F_2^{(1)}\\ G_2^{(1)}\end{bmatrix}e^{2i\pi\sigma_1 t_0}+\text{c.c.}+\begin{bmatrix}\Phi_0^{(1)}\\ F_0^{(1)}\\ G_0^{(1)}\end{bmatrix}, \tag{49}$$

where $\Phi_j^{(1)}$, $F_j^{(1)}$, and $G_j^{(1)}$ $(j=0,2)$ are functions of x and α to be determined, and the subscript j implies the coefficient of the jth harmonics, $e^{ij\pi\sigma_1 t_0}$. Substituting (49) into (45)–(47), we consider the respective harmonics separately. For the second harmonics, we eliminate $F_2^{(1)}$ and $G_2^{(1)}$ to derive the equation for $\Phi_2^{(1)}$ as follows:

$$\frac{d^2\Phi_2^{(1)}}{dx^2}+k_2^2\Phi_2^{(1)}=\frac{i}{2\pi\sigma_1}\{k_2^2\mathcal{A}_0+(k_2^2-4\pi^2)\mathcal{A}_2\times\cos[2\pi(x-1)]\}\alpha^2, \tag{50}$$

with $k_2^2=(2\pi\sigma_1)^2(1+\kappa s_2)$ and $s_2=\sigma_0^2/(\sigma_0^2-4\sigma_1^2)$ $(\sigma_1\neq\sigma_0/2)$, where $\mathcal{A}_0$ and $\mathcal{A}_2$ are given by

$$\mathcal{A}_0=\frac{\pi^2}{k_2^2}\left\{\gamma-3+\kappa\left[(s_1-s_2)\sigma_1^2-s_2+(\gamma-1)\times(s_1-1)s_1\sigma_1^2+4(\gamma-1)s_1^2s_2\frac{\sigma_1^2}{\Omega}\right]\right\}, \tag{51}$$

and

$$\mathcal{A}_2=\frac{\pi^2}{(k_2^2-4\pi^2)}\left\{\gamma+1+\kappa\left[(s_1-s_2)\sigma_1^2+s_2+(\gamma-1)\times(s_1-1)s_1\sigma_1^2+4(\gamma-1)s_1^2s_2\frac{\sigma_1^2}{\Omega}\right]\right\}, \tag{52}$$

with $\Omega=\sigma_0^2/\sigma_1^2$. Note that $k_2^2\neq4\pi^2$ but k_2 is assumed not to vanish, i.e., $\sigma_1\neq\sqrt{1+\kappa}\sigma_0/2$. The second-harmonic solutions are easily obtainable as

$$\Phi_2^{(1)}=\frac{i}{2\pi\sigma_1}\{\mathcal{A}_0+\mathcal{A}_2\cos[2\pi(x-1)]\}\alpha^2, \tag{53}$$

$$F_2^{(1)}=\left\{\mathcal{A}_0+\frac{1}{4}\left(1+\frac{1}{\sigma_1^2}\right)+\left[\mathcal{A}_2+\frac{1}{4}\left(1-\frac{1}{\sigma_1^2}\right)\right]\times\cos[2\pi(x-1)]\right\}\alpha^2, \tag{54}$$

$$G_2^{(1)}=\left\{s_2\left[\mathcal{A}_0+\frac{1}{4}\left(1+\frac{1}{\sigma_1^2}\right)-(\gamma-1)\frac{s_1^2}{\Omega}\right]+s_2\left[\mathcal{A}_2+\frac{1}{4}\left(1-\frac{1}{\sigma_1^2}\right)-(\gamma-1)\frac{s_1^2}{\Omega}\right]\cos[2\pi(x-1)]\right\}\alpha^2. \tag{55}$$

For the zeroth harmonics, on the other hand, the right-hand side of (45) contains no terms independent of t_0. Therefore, we take $\Phi_0^{(1)}=0$. From (46) and (47), we have

$$F_0^{(1)}=G_0^{(1)}=\left\{\frac{1}{2}\left(1-\frac{1}{\sigma_1^2}\right)+\frac{1}{2}\left(1+\frac{1}{\sigma_1^2}\right)\times\cos[2\pi(x-1)]\right\}|\alpha|^2. \tag{56}$$

These solutions show that while no steady streaming occurs at this order, the steady but nonuniform pressure distribution appears in the tube as well as in the cavities. The maximum $|\alpha|^2$ occurs at both ends, while the minimum $-|\alpha|^2/\sigma_1^2$ occurs in the middle. Note that the effect of the array, i.e., κ, appears only in the minimum through σ_1.

2. Second-order problem

Upon completion of the first-order problem, we proceed to the second-order problem. It is given by

$$\frac{\partial^2\phi^{(2)}}{\partial t_0^2}-\frac{\partial^2\phi^{(2)}}{\partial x^2}-\kappa\frac{\partial g^{(2)}}{\partial t_0}=K^{(2)}+L^{(2)}+M^{(2)}, \tag{57}$$

with

$$\begin{aligned}K^{(2)}=\kappa\Bigg\{&\frac{\partial g^{(0)}}{\partial t_2}-(\gamma-1)\frac{\partial}{\partial t_0}(g^{(0)}g^{(1)})\\&-(\gamma-2)\left(\frac{\partial\phi^{(0)}}{\partial t_0}\frac{\partial g^{(1)}}{\partial t_0}+\frac{\partial\phi^{(1)}}{\partial t_0}\frac{\partial g^{(0)}}{\partial t_0}\right)\\&-\frac{(\gamma-2)}{2}\left[\left(\frac{\partial\phi^{(0)}}{\partial t_0}\right)^2+\left(\frac{\partial\phi^{(0)}}{\partial x}\right)^2\right]\frac{\partial g^{(0)}}{\partial t_0}\\&+\frac{(\gamma-1)(\gamma-2)}{2}\frac{\partial\phi^{(0)}}{\partial t_0}\frac{\partial g^{(0)2}}{\partial t_0}\\&+\frac{(\gamma-1)(2\gamma-1)}{6}\frac{\partial g^{(0)3}}{\partial t_0}\Bigg\},\end{aligned} \tag{58}$$

$$L^{(2)}=-2\frac{\partial^2\phi^{(0)}}{\partial t_2\partial t_0}-\frac{\delta}{\varepsilon^2}\frac{\partial^{-1/2}}{\partial t_0^{-1/2}}\left(\frac{\partial^2\phi^{(0)}}{\partial x^2}\right), \tag{59}$$

$$\begin{aligned}M^{(2)}=&-\frac{\partial}{\partial t_0}\left(2\frac{\partial\phi^{(0)}}{\partial x}\frac{\partial\phi^{(1)}}{\partial x}\right)-(\gamma-1)\left(\frac{\partial\phi^{(0)}}{\partial t_0}\frac{\partial^2\phi^{(1)}}{\partial x^2}\right.\\&\left.+\frac{\partial\phi^{(1)}}{\partial t_0}\frac{\partial^2\phi^{(0)}}{\partial x^2}\right)-\frac{(\gamma+1)}{2}\left(\frac{\partial\phi^{(0)}}{\partial x}\right)^2\frac{\partial^2\phi^{(0)}}{\partial x^2},\end{aligned} \tag{60}$$

and

$$\begin{aligned}&\frac{\partial^2 g^{(2)}}{\partial t_0^2}+(\pi\sigma_0)^2g^{(2)}-(\pi\sigma_0)^2f^{(2)}\\&=-2\frac{\partial^2 g^{(0)}}{\partial t_2\partial t_0}-\frac{\delta_r}{\varepsilon^2}\frac{\partial^{3/2}g^{(0)}}{\partial t_0^{3/2}}+(\gamma-1)\frac{\partial^2}{\partial t_0^2}(g^{(0)}g^{(1)})\\&\quad-\frac{(\gamma-1)(2\gamma-1)}{6}\frac{\partial^2 g^{(0)3}}{\partial t_0^2},\end{aligned} \tag{61}$$

with

$$f^{(2)}=-\frac{\partial\phi^{(2)}}{\partial t_0}-\frac{\partial\phi^{(0)}}{\partial t_2}+\frac{\partial\phi^{(0)}}{\partial t_0}\frac{\partial\phi^{(1)}}{\partial t_0}-\frac{\partial\phi^{(0)}}{\partial x}\frac{\partial\phi^{(1)}}{\partial x}+\frac{(\gamma-2)}{6}\left(\frac{\partial\phi^{(0)}}{\partial t_0}\right)^3+\frac{1}{2}\frac{\partial\phi^{(0)}}{\partial t_0}\left(\frac{\partial\phi^{(0)}}{\partial x}\right)^2. \tag{62}$$

The boundary conditions now take

$$\frac{\partial\phi^{(2)}}{\partial x}=i\frac{E}{2\varepsilon^2}e^{i\pi\sigma_1 t_0}+\text{c.c. at } x=0, \tag{63}$$

and

$$\frac{\partial\phi^{(2)}}{\partial x}=0 \text{ at } x=1. \tag{64}$$

At this order, we do not necessarily have to seek the full solutions. We have only to derive the condition for the complex amplitude α from the boundary conditions. Setting the solutions in the following form:

$$\begin{bmatrix}\phi^{(2)}\\ f^{(2)}\\ g^{(2)}\end{bmatrix}=\begin{bmatrix}\Phi_1^{(2)}\\ F_1^{(2)}\\ G_1^{(2)}\end{bmatrix}e^{i\pi\sigma_1 t_0}+\begin{bmatrix}\Phi_3^{(2)}\\ F_3^{(2)}\\ G_3^{(2)}\end{bmatrix}e^{3i\pi\sigma_1 t_0}+\text{c.c.}, \tag{65}$$

and substituting this into (57)–(62), we end up with

$$\frac{d^2\Phi_1^{(2)}}{dx^2}+k_1^2\Phi_1^{(2)}=\mathcal{B}\cos[\pi(x-1)]+\text{terms in } \cos[3\pi(x-1)], \tag{66}$$

with $k_1^2=(\pi\sigma_1)^2(1+\kappa s_1)=\pi^2$ and

$$\mathcal{B}=-\mu\frac{\partial\alpha}{\partial t_2}+i\frac{S}{\varepsilon^2}\alpha+iQ_0|\alpha|^2\alpha, \tag{67}$$

where μ, S $(=S_{re}+iS_{im})$, and Q_0 $(=Q_1+Q_2+Q_3)$ are defined as

$$\mu=2+2\kappa s_1\left(1+\frac{s_1}{\Omega}\right)=\frac{2}{\pi\sigma_1}\frac{dk}{d\sigma}\bigg|_{\sigma=\sigma_1}, \tag{68}$$

$$S_{re}=-S_{im}=-\sqrt{\frac{\pi\sigma_1}{2}}\left(\frac{\delta}{\sigma_1^2}+\frac{\kappa\delta_r s_1^2}{\Omega}\right), \tag{69}$$

$$Q_1=-\frac{\pi}{\sigma_1}\left\{\gamma-1+\kappa\sigma_1^2\left[-(\gamma-3)s_1+2(\gamma-2)s_2-(\gamma-1)s_1s_2-(\gamma-1)\frac{s_1^2s_2}{\Omega}\right]\right\}\mathcal{A}_0, \tag{70}$$

$$Q_2=\frac{\pi}{2\sigma_1}\left\{\gamma+1-\kappa\sigma_1^2\left[-\left(\gamma-3+\frac{1}{\sigma_1^2}\right)s_1+2(\gamma-2)s_2-(\gamma-1)s_1s_2-(\gamma-1)\frac{s_1^2s_2}{\Omega}\right]\right\}\mathcal{A}_2, \tag{71}$$

and

$$Q_3=-\frac{3\pi(\gamma+1)}{8\sigma_1^3}+\frac{\pi\kappa\sigma_1}{8}\left\{\left[6(2\gamma-3)+\frac{(\gamma-3)}{\sigma_1^2}\right]s_1-2(\gamma-2)\left(3+\frac{1}{\sigma_1^2}\right)s_2\right\}+\frac{\pi\kappa\sigma_1(\gamma-1)}{8}\left\{6(\gamma-2)s_1^2+\left(3+\frac{1}{\sigma_1^2}\right)s_1s_2-3(2\gamma-1)s_1^3+\left[2\left(3-\frac{1}{\sigma_1^2}\right)+24(\gamma-2)s_2+\left(3+\frac{1}{\sigma_1^2}\right)s_2-3(2\gamma-1)s_1^2-12(\gamma-1)\left(1+\frac{s_1}{\Omega}\right)s_1s_2\right]\frac{s_1^2}{\Omega}\right\}. \tag{72}$$

Here, note that the fractional derivative of minus half-order of the exponential function is reduced to the Fresnel integral[11] and given simply as

$$\frac{\partial^{-1/2}}{\partial t_0^{-1/2}}e^{i\pi\sigma_1 t_0}=\frac{(1-i)}{\sqrt{2\pi\sigma_1}}e^{i\pi\sigma_1 t_0}=(i\pi\sigma_1)^{-1/2}e^{i\pi\sigma_1 t_0}. \tag{73}$$

The derivative of three-half order is given by $-(1-i)\times(\pi\sigma_1)^2/\sqrt{2\pi\sigma_1}\exp(i\pi\sigma_1 t_0)$ $[=(i\pi\sigma_1)^{3/2}\exp(i\pi\sigma_1 t_0)]$. It is found from (69) that since κ is small, the friction loss due to the throat wall becomes comparably small with the one due to the tube wall. In addition, when Ω is chosen large, it is made even smaller.

The solution $\Phi_1^{(2)}$ is obtained as

$$\Phi_1^{(2)}=\frac{\mathcal{B}}{2\pi}(x-1)\sin[\pi(x-1)]+\mathcal{C}_1\cos[\pi(x-1)]+\mathcal{C}_2\sin[\pi(x-1)]+\text{terms in}\cos[3\pi(x-1)], \tag{74}$$

where $\mathcal{C}_1$ and $\mathcal{C}_2$ are integration constants to be determined. By imposing the boundary conditions (63) and (64), it follows that while $\mathcal{C}_1$, i.e., the coefficient of the homogeneous solution, is left undetermined within the present framework of the theory,[12] $\mathcal{C}_2$ must vanish, and $\mathcal{B}=iE/\varepsilon^2$. The latter gives the equation governing the behavior of α as

$$i\mu\frac{\partial\alpha}{\partial t_2}+\frac{S}{\varepsilon^2}\alpha+Q_0|\alpha|^2\alpha=\frac{E}{\varepsilon^2}. \tag{75}$$

Here, we examine the value of Q_0 for a large value of Ω. Noting that $s_1=1/(1-1/\Omega)\approx 1+1/\Omega+\cdots$ and $s_2=1/(1-4/\Omega)\approx 1+4/\Omega+\cdots$ so that $s_2-s_1\ll 1$, and $k_2^2=4\pi^2[1+\kappa(s_2-s_1)\sigma_1^2]$, it is found that $\mathcal{A}_2$ is much larger than the other terms and therefore Q_2 is dominant in Q_0. Approximating $\mathcal{A}_2$ to be

$$\mathcal{A}_2\approx\frac{\pi^2(\gamma+1+\kappa)}{(k_2^2-4\pi^2)}, \tag{76}$$

Q_0 may be evaluated as

$$Q_0\approx Q_2\approx\frac{\pi^3(\gamma+1+\kappa)^2}{2\sigma_1(k_2^2-4\pi^2)}>0. \tag{77}$$

Thus, it is found that Q_0 is positive for $\Omega\gg 1$.

We proceed to complete the second-order problem by taking account of all terms including those unspecified so far. Although the calculations are straightforward, the full expressions for $\phi^{(2)}$, $f^{(2)}$, $g^{(2)}$ are too complicated to be reproduced here. By making use of the same approximation leading to (76), we present here only the leading expressions for the respective modes

$$\Phi_1^{(2)} \approx -\frac{i(\gamma-3-\kappa)}{16\pi\sigma_1}\mathcal{A}_2 \cos[3\pi(x-1)]|\alpha|^2\alpha, \tag{78}$$

$$\Phi_3^{(2)} \approx \frac{3i\pi(\gamma-3-\kappa)}{2\sigma_1(k_3^2-\pi^2)}\mathcal{A}_2 \cos[\pi(x-1)]\alpha^3 + \frac{3i\pi(\gamma+1+\kappa)}{2\sigma_1(k_3^2-9\pi^2)}\mathcal{A}_2 \cos[3\pi(x-1)]\alpha^3, \tag{79}$$

$$F_1^{(2)} \approx -\frac{i}{\pi\sigma_1}\frac{\partial\alpha}{\partial t_2}\cos[\pi(x-1)] + \frac{1}{2}\left(1-\frac{1}{\sigma_1^2}\right)\mathcal{A}_2 \times \cos[\pi(x-1)]|\alpha|^2\alpha - \left[\frac{(\gamma-3-\kappa)}{16} - \frac{1}{2}\left(1+\frac{1}{\sigma_1^2}\right)\right]\mathcal{A}_2 \cos[3\pi(x-1)]|\alpha|^2\alpha, \tag{80}$$

$$F_3^{(2)} \approx \left[\frac{9\pi^2(\gamma-3-\kappa)}{2(k_3^2-\pi^2)} + \frac{1}{2}\left(1+\frac{1}{\sigma_1^2}\right)\right]\mathcal{A}_2 \cos[\pi(x-1)]\alpha^3 + \frac{9\pi^2(\gamma+1+\kappa)}{2(k_3^2-9\pi^2)}\mathcal{A}_2 \cos[3\pi(x-1)]\alpha^3, \tag{81}$$

$$G_1^{(2)} \approx s_1 F_1^{(2)}, \tag{82}$$

$$G_3^{(2)} \approx s_3 F_3^{(2)}, \tag{83}$$

with $k_3^2=(3\pi\sigma_1)^2(1+\kappa s_3)\neq 9\pi^2$ and $s_3=\sigma_0^2/(\sigma_0^2-9\sigma_1^2)$, where the approximation (76) is used, and s_1 and s_3 in $G_1^{(2)}$ and $G_3^{(2)}$ are left unapproximated. Here, we assume that $k_3^2 \neq \pi^2$ and $\sigma_1 \neq \sigma_0/3$. Details will be discussed later.

B. Steady-state solution

Let us examine the steady-state solution to (75). Before doing this, we transform the equation into a form suitable for comparison with the results of measurements. So far ε has been used conveniently to make a note of ordering in developing the asymptotic analysis. From the viewpoint of the experiment, however, it is not a quantity to be measured easily, while use of α is not also suitable for comparison. Because an available quantity is the excess pressure in the tube, we rewrite (75) in terms of the dimensionless excess pressure relative to p_0. In view of (18), (42), and (44), we set

$$\frac{\rho_0 a_0 u_0 \overline{p}'}{p_0} = \varepsilon\gamma\overline{p}' = \frac{1}{2}\cos[\pi(x-1)]P e^{i\pi\sigma_1 t} + \text{c.c.} + \cdots, \tag{84}$$

where $P=2\varepsilon\gamma\alpha$ ($\ll 1$) to the lowest order. Noting that $\partial\alpha/\partial t=\varepsilon^2\partial\alpha/\partial t_2+\cdots$, and using P instead of α, (75) is rewritten as

$$i\mu\frac{\partial P}{\partial t} + SP + Q|P|^2P = \Gamma e^{i\pi\Delta\sigma t}, \tag{85}$$

with $Q=Q_0/4\gamma^2$, $\Gamma=2\pi\gamma\sigma_1 c$, and $\Delta\sigma=\varepsilon^2\sigma'$.

Setting $P=|P|\exp(i\theta)$ and separating the real and imaginary parts, it follows that

$$\mu\frac{\partial|P|}{\partial t} + S_{im}|P| = \Gamma\sin\psi, \tag{86}$$

and

$$\mu|P|\frac{\partial\psi}{\partial t} - \pi\mu\Delta\sigma|P| + S_{re}|P| + Q|P|^3 = \Gamma\cos\psi, \tag{87}$$

with $\psi=\pi\Delta\sigma t-\theta$. For the steady-state solution, we drop $\partial/\partial t$ to have $S_{im}|P|=\Gamma\sin\psi$, $\theta=\pi\Delta\sigma t+\text{constant}$, and

$$\Delta\sigma = \frac{1}{\pi\mu}\left(S_{re} + Q|P|^2 \pm \sqrt{\frac{\Gamma^2}{|P|^2} - S_{im}^2}\right). \tag{88}$$

It is found that $|P|$ is bounded at Γ/S_{im}. This suggests that the peak amplitude is proportional to the magnitude of excitation Γ, i.e., c. It is also found that the peak frequency is shifted downward by the dispersion due to the wall friction while shifted upward by nonlinearity, because $S_{re}<0$ and $Q>0$ for $\Omega\gg 1$. If $\Gamma\ll 1$ so that $|P|\ll 1$, we can neglect $Q|P|^2P$ in (85) to have immediately the steady-state solution as

$$P = \frac{\Gamma e^{i\pi\Delta\sigma t}}{S-\pi\mu\Delta\sigma}. \tag{89}$$

Thus, we obtain the linear resonance curve given by

$$|P| = \frac{\Gamma}{\sqrt{(\pi\mu\Delta\sigma - S_{re})^2 + S_{im}^2}}, \tag{90}$$

which is consistent with (88) in the limit as $P\to 0$.

Incidentally, (90) can also be derived from the linear theory shown previously.[4] When the lossy effects are included, the form of p' in (36) is unaltered but k^2 is modified as

$$k^2 = \pi^2\sigma^2\left\{\frac{1+\kappa\sigma_0^2/[\sigma_0^2-\sigma^2-(1-i)\delta_r\sigma^2/\sqrt{2\pi\sigma}]}{1-(1-i)\delta/\sqrt{2\pi\sigma}}\right\}. \tag{91}$$

See the expression for k below (4) in Ref. 4. But, note the difference in the sign of argument of the exponential function for the piston displacement. This difference yields $-i$ instead of $+i$. Expanding the right-hand side of (91) around $\sigma=\sigma_0$ by setting $\sigma=\sigma_1+\Delta\sigma$, we retain the lossless terms up to the order of $\Delta\sigma$ but truncate the lossy terms to the lowest order. Thus, k is obtained as $\pi+(\pi\mu\Delta\sigma-S)\sigma_1/2$. Next, noting that α in (44) corresponds to $(\pi^2\sigma^2/k\sin k)c/2\varepsilon$, we approximate $k\sin k$ as $-\pi(k-\pi)$ and take the lowest terms for α to recover (90) after multiplying it by $2\varepsilon\gamma$ in the relation between α and P.

V. DISCUSSION OF THE RESULTS

A. Nonlinear frequency response

The nonlinear frequency response in the steady state is described by (88) theoretically. The peak amplitude P_{peak} attained in the response curve is determined to be Γ/S_{im} by the linear loss, while the peak frequency at $P=P_{\text{peak}}$ is lowered by $\Delta\sigma=S_{re}/\pi\mu$ due to the dispersive effects of the boundary layer. This result is merely an extension of the linear case. Although the linear downshift is constant, the shift dependent on the amplitude occurs through $Q|P|^2P$, which is responsible for bending (skew) of the response curve toward the higher or lower frequency side. We examine variations of Q as σ_0 is changed with κ fixed. This corresponds physically to changing cavity volume and axial spacing, with the tube length, its cross-sectional area, and the throat length held constant.

From (70)–(72) with (51) and (52), it is expected that Q may diverge at (i) $|s_1|=\infty$; (ii) $|s_2|=\infty$; (iii) $k_2^2=0$; or (iv) $k_2^2=4\pi^2$. The first case (i) where $\sigma_1=\sigma_0$ does not occur unless $\kappa=0$ or $\sigma_0=0$, as is seen from Fig. 2(a) or (37). The second case (ii) with $2\sigma_1=\sigma_0$ may occur if the frequency of the second harmonics hits σ_0, whereby σ_0 and κ must satisfy the relation $\sigma_0=\sqrt{12/(3+4\kappa)}$. But, because of evanescence at σ_0, no divergence of Q occurs there. In fact, it is confirmed that all terms proportional to s_2 in Q cancel out altogether. The third case (iii) corresponds to the one with $2\sigma_1=\sqrt{1+\kappa}\sigma_0$ for resonance, and indeed occurs when σ_0 and κ satisfy the following relation:

$$\sigma_0=\sqrt{\frac{4(3-\kappa)}{3(1+\kappa)^2}}\equiv\sigma_{cr}<2. \tag{92}$$

The fourth case (iv) corresponds to the second harmonic resonance when $2\sigma_1$ hits $2\sigma^{\pm}$. But this case does not occur because $\sigma_1\neq 0$ nor $\sigma_1\neq 1$. Besides the third case, Q diverges in the limit as $\sigma_0\to 0$. This divergence is very rapid as $-\pi(\gamma-1)(2\gamma+1)/32\gamma^2\kappa^3\sigma_0^7$. In addition, we have assumed for the second-order solutions that $k_3^2\neq\pi^2$ or $\sigma_1\neq\sigma_0/3$. The equality $k_3^2=\pi^2$ holds for $\sigma_1=\sqrt{\sigma_0/3}$, where $\sigma_0=(5\pm\sqrt{16-9\kappa})/3(1+\kappa)$. The equality $\sigma_1=\sigma_0/3$ holds for $\sigma_0=\sqrt{72/(8+9\kappa)}$. Although these cases have no direct bearing on (85), they should be avoided in the sense of seeking uniformly valid, asymptotic solutions.

Taking account of such exceptional cases, Q is drawn versus σ_0 in Fig. 3(a) for three fixed values of κ. The broken, solid, and dotted lines represent the values of Q for $\kappa=0.1$, 0.2, and 0.3, respectively. As is seen, Q takes both positive and negative values. This means that the response curve may be bent rightward or leftward, depending on the choice of σ_0. While Q diverges at $\sigma_0=\sigma_{cr}$ and at $\sigma_0=0$, it grows as σ_0 increases. In this limit, the asymptotic expression (77) for Q_0 is already available so that Q is approximated as

$$Q=\frac{Q_0}{4\gamma^2}\approx Q_a=\frac{\pi^3(\gamma+1+\kappa)^2}{8\gamma^2\sigma_1(k_2^2-4\pi^2)}. \tag{93}$$

Figure 3(b) shows the relative error $|(Q-Q_a)/Q|$ for three values of $\kappa=0.1$, 0.2, and 0.3 by using the same types of lines as in Fig. 3(a). It is found that Q_a agrees with Q very well for $\sigma>2$ and the relative errors are almost less than 1%. Even below σ_{cr}, there is a region in which Q_a still gives a good approximation to Q.

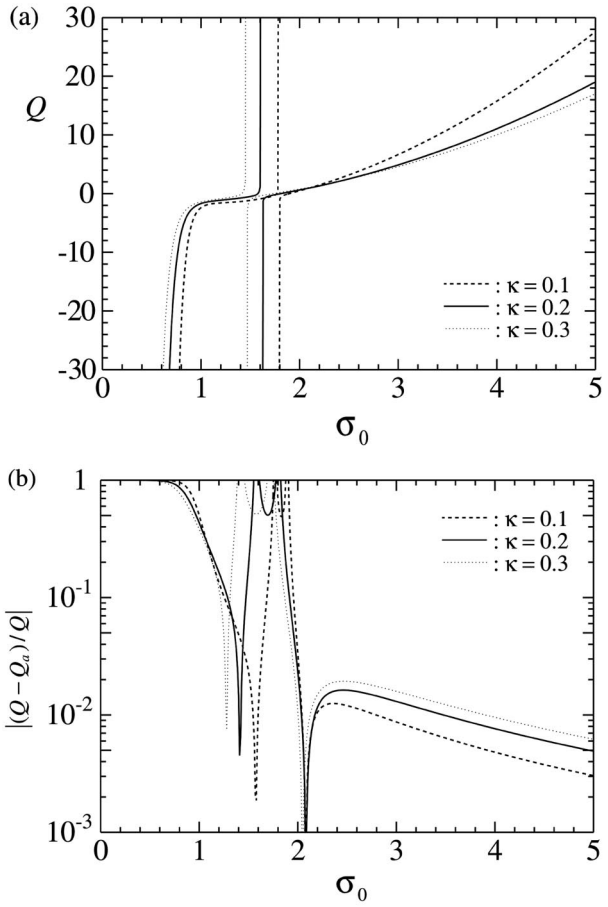

FIG. 3. Graphs of the coefficient Q versus σ_0 with κ fixed at 0.1, 0.2 and 0.3: (a) displays the values of Q where the respective values diverge at $\sigma_0=\sigma_{cr}\approx 1.79$, 1.61, and 1.46 and at $\sigma_0=0$, and (b) displays the relative errors $|(Q-Q_a)/Q|$ of the asymptotic values Q_a to Q for the three values of κ.

The other parameters μ and S are relatively simple. Figure 4 displays the graphs of μ and S_{im} versus σ_0 for $\kappa=0.1$, 0.2, and 0.3, where the meaning of D will be given later. Three families of curves labeled μ, S_{im}, and D are drawn. In each family, the broken, solid, and dotted lines represent the values of labeled quantity for $\kappa=0.1$, 0.2, and 0.3, respectively. In order to draw the graphs of S_{im}, the values of δ and δ_r are set to be 0.0282 and 0.223 in view of the experiment to be decribed in the next subsection. The value of δ_r is a little larger than the estimation. It is found that all quantities decrease as σ_0 increases, but they are almost constant for $\sigma>2$, and they decrease as κ becomes smaller.

B. Comparison with the experimental result

We now compare the frequency response with the one measured by using the tube of length l ($=3256$ mm) and of diameter $2R$ ($=80$ mm) with the Helmholtz resonator having a cavity of volume V ($=49.7\times10^{-6}$ m^3), and a throat of length L ($=35.6$ mm) and of diameter $2r$ ($=7.11$ mm) con-

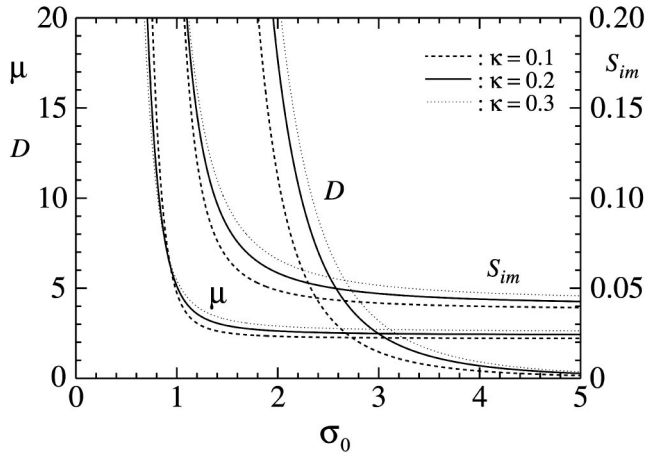

FIG. 4. Graphs of the coefficients μ, S_{im}, and D vs σ_0 for $\kappa=0.1$, 0.2, and 0.3.

nected with the axial spacing d ($=50$ mm). The size parameter κ takes the value 0.198. Figure 5 is the reproduction of the frequency response reported in Ref. 4 (see Fig. 4), where the half of the peak-to-peak value of the excess pressure measured on the flat plate at the closed end, δp, relative to the atmospheric pressure p_0 is drawn versus the frequency of excitation $\omega/2\pi$. The blank triangle, solid triangle, blank circle, and solid circle indicate the data measured at the displacement amplitude of the bellows $X_b=0.5$, 1.5, 2.5, and 3.5 mm, respectively. The equilibrium pressure and the mean temperature in the tube near the closed end are 1.007×10^5 Pa and 25.6 °C, respectively, so $a_0=347.1$ m/s, $\nu=1.567\times10^{-5}$ m^2/s, Pr$=0.7089$, and $\gamma=1.402$. At this temperature, the natural frequency of the resonator $\omega_0/2\pi$ is calculated to be 242.6 Hz with the end corrections. Thus, we find that $\sigma_0=4.55$ and $\sigma_1=0.911$.

Since $\kappa=0.198$ and $\sigma_0=4.55$ for the experiment, we have $\mu=2.43$, $Q=15.2$, $-S_{re}=S_{im}=0.0430$. In Fig. 5, the

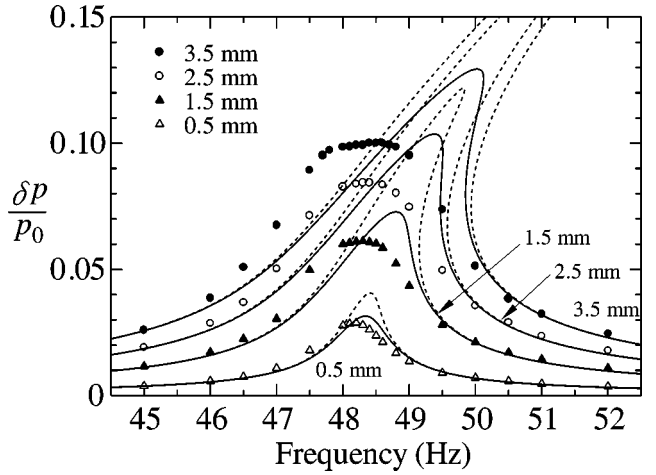

FIG. 5. Comparison of the nonlinear frequency response obtained by the theory and experiment for the displacement amplitude of the bellows $X_b \geqslant 0.5$ mm, where the broken and solid lines represent, respectively, the curves without taking account of the jet loss and with it, while the measured data are indicated by the blank triangle, solid triangle, blank circle, and solid circle for $X_b=0.5$, 1.5, 2.5, and 3.5 mm, respectively, X_b being related to the one of the piston by $X_p=1.422X_b$.

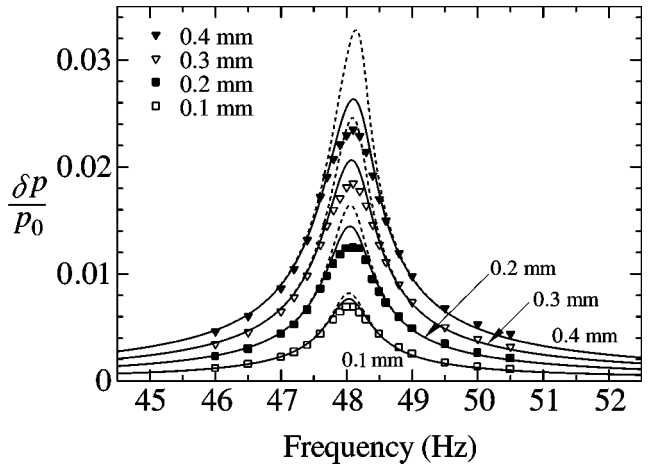

FIG. 6. Comparison of the nonlinear frequency response obtained by the theory and experiment for the displacement amplitude of the bellows $X_b<0.5$ mm, where the broken and solid lines represent, respectively, the curves without taking account of the jet loss and with it, while the measured data are indicated by the blank square, solid square, blank triangle, and solid triangle for $X_b=0.1$, 0.2, 0.3, and 0.4 mm, respectively, X_b being related to the one of the piston by $X_p=1.422X_b$.

broken lines represent $|P|$ versus the dimensional frequency $(\sigma_1+\Delta\sigma)a_0/2l$ by using (88). The displacement of the bellows is converted into the one of the piston by multiplying it with a factor 1.422,[4] so that Γ is given by $2\pi\gamma\sigma_1 X_p/l$ with $X_p=1.422X_b$. The theory overestimates not only the peak amplitudes but also the peak frequencies considerably, even for $X_b=0.5$ mm. When higher-order corrections to p' in $|P|$ on the right-hand side of (84) are taken into account, it is found that the deviation becomes worse. This is understood from the nature of asymptotic expansions that inclusion of higher-order terms does not necessarily improve the accuracy. Rather, the smallness of $|P|$ is required. Hence, it turns out that the theory based on (88) fails to describe the experimental results adequately.

So, the experimental data for X_b smaller than 0.5 mm are presented, though unpublished so far. Figure 6 shows the frequency response where the blank square, solid square, blank triangle, and solid triangle indicate the data measured at $X_b=0.1$, 0.2, 0.3, and 0.4 mm, respectively, and the equilibrium pressure and the mean temperature are 1.010×10^5 Pa and 23.1 °C, respectively. As in Fig. 5, the broken lines represent $|P|$ versus the dimensional frequency calculated by (88) where $a_0=345.6$ m/s, $\nu=1.539\times10^{-5}$ m^2/s, Pr$=0.7095$, and $\gamma=1.402$. While $\omega_0/2\pi$ is now shifted to be 241.3 Hz, note that both σ_0 and σ_1 are independent of a_0 and therefore of the temperature. It is seen in Fig. 6 that as X_b is decreased, the broken lines tend to approach the data measured. But, the theory overestimates the peak amplitude slightly even for the smallest excitation with $X_b=0.1$ mm.

C. Effect of jet loss

The discrepancy may be attributed to some effects not taken into account in the analysis. One is an effect of jet loss which occurs at the throat of the resonator. As the amplitude of oscillatory flows in the throat becomes large, the flow pattern (except for direction of flow) just entering the throat

differs from the one leaving the throat (see Fig. 1). When the air is sucked into the throat, it flows toward the orifice omnidirectionally, whereas when it is ejected, it flows in the form of jet unidirectionally. This asymmetry of flow pattern on the suction and ejection sides gives rise to the jet loss. The detailed analysis is given in the Appendix of Ref. 10 and is not reproduced here. The jet loss introduces the additional term

$$-\frac{V}{\rho_0 a_0^2 B L_e}\left|\frac{\partial p_c'}{\partial t}\right|\frac{\partial p_c'}{\partial t}, \tag{94}$$

to the right-hand side of (9) for the behavior of the resonator. Then, the normalized equation (24) is modified into

$$\frac{\partial^2 \overline{p_c'}}{\partial \overline{t}^2}+\delta_r\frac{\partial^{3/2}\overline{p_c'}}{\partial \overline{t}^{3/2}}+(\pi\sigma_0)^2\overline{p_c'}$$
$$=(\pi\sigma_0)^2\overline{p'}+\varepsilon\frac{(\gamma-1)}{2}\frac{\partial^2\overline{p_c'}^2}{\partial\overline{t}^2}$$
$$-\varepsilon^2\frac{(\gamma-1)(2\gamma-1)}{6}\frac{\partial^2\overline{p_c'}^3}{\partial\overline{t}^2}-\varepsilon\delta_J\left|\frac{\partial\overline{p_c'}}{\partial\overline{t}}\right|\frac{\partial\overline{p_c'}}{\partial\overline{t}}, \tag{95}$$

where $\delta_J=V/BL_e=(l/\pi\sigma_0 L_e)^2$. Since the new term is accompanied by ε, it yields additional terms in the first-order solution. In fact, it follows that

$$\left|\frac{\partial g^{(0)}}{\partial t_0}\right|\frac{\partial g^{(0)}}{\partial t_0}=-4(\pi\sigma_1 s_1)^2(|\sin\xi|\sin\xi)\{|\cos[\pi(x-1)]|$$
$$\times\cos[\pi(x-1)]\}|\alpha|^2, \tag{96}$$

with $\alpha=|\alpha|e^{i\theta}$ and $\xi=\pi\sigma_1 t_0+\theta$. Using the following Fourier expansions:

$$|\sin\xi|\sin\xi=-\frac{2i}{\pi}\sum_{n=-\infty}^{\infty}\frac{[(-1)^n-1]}{n(n^2-4)}e^{in\xi}$$
$$=-\frac{4i}{3\pi}e^{i\xi}+\frac{4i}{15\pi}e^{3i\xi}+\cdots+\text{c.c.}, \tag{97}$$

and

$$|\cos[\pi(x-1)]|\cos[\pi(x-1)]$$
$$=-\frac{4}{\pi}\sum_{n=-\infty}^{\infty}\frac{\sin(n\pi/2)}{n(n^2-4)}e^{in\eta}$$
$$=\frac{8}{3\pi}\cos[\pi(x-1)]+\frac{8}{15\pi}\cos 3[\pi(x-1)]+\cdots, \tag{98}$$

with $\pi x=\eta$ and the sums taken except for $n=0$ and $n=\pm 2$, there arises in (46) the term proportional to $\cos[\pi(x-1)]\exp(i\pi\sigma_1 t_0)|\alpha|\alpha$. Note that although $\cos[\pi(x-1)]$ is defined only in the interval $0\leqslant x\leqslant 1$ originally, it is extended periodically to the outside of it with period 2 and so is the case with $|\cos[\pi(x-1)]|$. Thus, the solution (49) must include the component $\Phi_1^{(1)}\exp(i\pi\sigma_1 t_0)$. As is inferred from the analysis for the second-order problem, this term gives rise to the equation for $\Phi_1^{(1)}$ corresponding to (66) with $\mathcal{B}$ proportional to $|\alpha|\alpha$. Applying the boundary conditions (48), it follows that α must vanish. To remedy this, it may be considered to introduce another time variable $t_1(\equiv\varepsilon t)$. But, as $\Delta\sigma$ and E are assumed to be of order ε^2, the introduction of t_1 is inconsistent.

To resolve the dilemma, we notice the following point. The parameter κ takes a small value such as 0.1 or 0.2, but it has been regarded as a quantity of order unity and independent of ε. As the magnitude of ε becomes comparable with the value of κ, however, the smallness of the latter may be taken into account. If κ is taken as small as ε, the contribution from the jet loss had rather be incorporated in the second-order problem. Then, $\mathcal{B}$ in (67) includes the additional term given by

$$-\frac{128\kappa\delta_J\sigma_1^3 s_1^3}{9\pi\varepsilon\sigma_0^2}|\alpha|\alpha, \tag{99}$$

and (75) is replaced by

$$i\mu\frac{\partial\alpha}{\partial t_2}+\frac{S}{\varepsilon^2}\alpha+i\frac{D_0}{\varepsilon}|\alpha|\alpha+Q_0|\alpha|^2\alpha=\sigma_1\frac{E}{\varepsilon^2}, \tag{100}$$

with $D_0=128\kappa\delta_J\sigma_1^3 s_1^3/9\pi\sigma_0^2$. In terms of P, finally, (85) is modified as

$$i\mu\frac{\partial P}{\partial t}+SP+iD|P|P+Q|P|^2P=\Gamma e^{i\pi\Delta\sigma t}, \tag{101}$$

with

$$D=\frac{64\kappa\delta_J\sigma_1 s_1^3}{9\pi\gamma\Omega}. \tag{102}$$

In Fig. 4, the graph of D vs σ_0 is displayed for $\kappa=0.1$, 0.2, and 0.3.

Separating the real and imaginary parts of (101) by setting $P=|P|\exp(i\theta)$, the only correction to (86) and (87) is to replace S_{im} with $S_{im}+D|P|$. Then, the frequency response is given by

$$\Delta\sigma=\frac{1}{\pi\mu}\left[S_{re}+Q|P|^2\pm\sqrt{\frac{\Gamma^2}{|P|^2}-(S_{im}+D|P|)^2}\right]. \tag{103}$$

It is found that the jet loss adds $D|P|$ to the linear one S_{im}, and then the peak amplitude is determined as

$$P_{\text{peak}}=\frac{1}{2D}(-S_{im}+\sqrt{S_{im}^2+4D\Gamma}). \tag{104}$$

For $\Gamma\ll S_{im}^2/4D$, P_{peak} is given by Γ/S_{im}, whereas for $\Gamma\gg S_{im}^2/4D$, P_{peak} is given by $\sqrt{\Gamma/D}$. The latter suggests that the peak amplitude does not increase in proportion to Γ as in the linear regime but to $\sqrt{\Gamma}$. The changeover may be defined to occur at $\Gamma=S_{im}^2/4D\equiv\Gamma_{ch}$, which gives $\Gamma_{ch}=0.0012$ for $D=0.398$. This corresponds to 0.34 mm for X_b.

The response curves taking account of the jet loss are drawn in the solid lines in Fig. 5. For the amplitude 0.5 mm, good agreement is observed for the peak amplitude but the peak frequency is slightly overestimated. The latter is determined by the accuracy of measurement of the temperature. If the temperature is higher by 1 degree, then the peak frequency is shifted by 0.09 Hz to the right. For the amplitude smaller than 0.5 mm, the solid lines in Fig. 6 shows the

response curves with the jet loss. In this case, the peak frequencies are well predicted. Although the peak amplitudes are overestimated slightly, it is found that account of the jet loss iproves the results considerably.

As the amplitude increases beyond 0.5 mm, however, there arises significant discrepancy. It may be attributed to the following two points. Although the frequency of the second harmonics never hits σ_2^-, the ratio σ_2^-/σ_1 is 1.98 and very close to 2 numerically. Even if no shock then occurs, this situation is not preferable to the theory. Secondly, the frequency of the fifth harmonics, $5\sigma_1$, hits σ_0 for evanescence in the present case. Then the energy absorption at the fifth harmonics is enhanced so that the theory might be limited. Furthermore if causes of the discrepancy are sought beyond the present framework, it is open whether or not the weakly nonlinear theory is still applicable. In addition, another effect of transverse motions of air in the cross-section might come into play, associated with emergence of acoustic streaming. To make a firm conclusion, however, it is necessary to check validity of the theory against new experiments by using tubes in geometrically different configuration taking account of some restrictions.

VI. CONCLUSIONS

The weakly nonlinear theory has been developed to obtain the frequency response of forced oscillations of the air column in the closed tube with the array of Helmholtz resonators connected axially. Since the array introduces the wave dispersion, shock-free, high-amplitude oscillations are obtainable, and for their analysis, the usual asymptotic method of multiple is successfully applicable. The analysis is based on the assumptions of one-dimensional motions in the acoustic main flow outside of the boundary layer on the tube wall, and of the continuum approximation of the discrete distribution of the resonators. Thus, no acoustic streaming involving transverse motions of air in the cross section is covered, but the steady but axially nonuniform pressure distribution of quadratic order is revealed. By completing the second-order problem, the cubic nonlinear equation describing temporal slow modulation of the complex pressure amplitude of the lowest mode has been derived.

In the linear regime, as is well known, the small dissipation and dispersion caused by the boundary layer on the tube and throat wall limit the peak amplitude and lower the peak frequency. As the amplitude of excitation is increased, the nonlinear frequency shift occurs, depending on the amplitude of oscillations and on the natural frequency of the resonator. The shift is crucially determined by the coefficient Q in the equation. It takes positive or negative values so that the response curve may be bent toward the high- or low-frequency side. But, it is usual that Q is positive and the response curve is bent toward the high-frequency side, because the natural frequency of resonator is chosen higher than the critical frequency σ_{cr}. When the theoretical curve is compared with the experiment, it is revealed that both results do not agree with each other quantitatively, although qualitatively the tendency of the bent may be explained. In particular, the theory overestimates the peak amplitude considerably.

The discrepancy has been resolved to some extent by taking account of the jet loss at the throat. It introduces the additional nonlinear dissipation to the linear one so that the peak amplitude is suppressed as the amplitude becomes large. It is found that the peak amplitude then becomes proportional to the square root of the amplitude of excitation. As far as the present experiment is concerned, the linear and weakly nonlinear theory with the jet loss can give a quantitative description up to the pressure amplitude 3% to the equilibrium pressure. In order to design a tube for generation of even higher peak amplitude, the results in the present paper provide useful guidelines.

ACKNOWLEDGMENTS

The authors acknowledge the support by the Grants-in-Aid from the Japan Society of Promotion of Science and also from The Mitsubishi Foundations, Tokyo, Japan.

[1] A. B. Coppens and A. A. Atchley, ''Nonlinear standing waves in cavities,'' in *Encyclopedia of Acoustics*, edited M. J. Crocker (Wiley, New York, 1997), Vol. 1, pp. 237–247.

[2] C. C. Lawrenson, B. Lipkens, T. S. Lucas, D. K. Perkins, and T. W. Van Doren, ''Measurements of macrosonic standing waves in oscillating closed cavities,'' J. Acoust. Soc. Am. **104**, 623–636 (1998).

[3] Y. A. Ilinskii, B. Lipkens, T. S. Lucas, T. W. Van Doren, and E. A. Zabolotskaya, ''Nonlinear standing waves in an acoustical resonator,'' J. Acoust. Soc. Am. **104**, 2664–2674 (1998).

[4] N. Sugimoto, M. Masuda, T. Hashiguchi, and T. Doi, ''Annihilation of shocks in forced oscillations of an air column in a closed tube,'' J. Acoust. Soc. Am. **110**, 2263–2266 (2001).

[5] N. Sugimoto, ''Emergence of an acoustic shock wave in a tunnel and a concept of shock-free propagation,'' in *Noise and Vibration from High-Speed Trains*, edited V. V. Krylov (Thomas Telford, London, 2001), pp. 213–247.

[6] O. V. Rudenko, ''Artificial nonlinear media with a resonant absorber,'' Sov. Phys. Acoust. **29**, 234–237 (1983).

[7] V. G. Andreev, V. E. Gusev, A. A. Karabutov, O. V. Rudenko, and O. A. Sapozhnikov, ''Enhancement of the Q of a nonlinear acoustic resonator by means of a selectively absorbing mirror,'' Sov. Phys. Acoust. **31**, 162–163 (1985).

[8] V. E. Gusev, H. Bailliet, P. Lotton, S. Job, and M. Bruneau, ''Enhancement of the Q of a nonlinear acoustic resonator by active suppression of harmonics,'' J. Acoust. Soc. Am. **103**, 3717–3720 (1998).

[9] J. Kevorkian and J. D. Cole, *Multiple Scale and Singular Perturbation Methods* (Springer, New York, 1996).

[10] N. Sugimoto, ''Propagation of nonlinear acoustic waves in a tunnel with an array of Helmholtz resonators,'' J. Fluid Mech. **244**, 55–78 (1992).

[11] M. Abramowitz and I. A. Stegun, *Handbook of Mathematical Functions* (Dover, New York, 1972).

[12] Although C_1 should be determined, in nature, by solving an initial-value problem from start-up, it may be set equal to zero if the combination $\alpha - \varepsilon^2 i\pi\sigma_1 C_1$ on substitution of the solutions obtained into (42) is replaced by α newly. Then, (75) [and (100)] are rewritten in terms of this new α but their form is subjected to no alterations within the order concerned.